Facially Amphipathic Glycopolymers Inhibit Ice Recrystallization

Ben Graham, Alice E. R. Fayter, Judith E. Houston, Rachel C. Evans, and Matthew I. Gibson

J. Am. Chem. Soc., **Just Accepted Manuscript** • DOI: 10.1021/jacs.8b02066 • Publication Date (Web): 16 Apr 2018

Facially Amphipathic Glycopolymers Inhibit Ice Recrystallization

Ben Graham,[1] Alice E. R. Fayter,[1] Judith E. Houston,[3] Rachel C. Evans,[4] and Matthew I. Gibson[1,2]*

[1] Department of Chemistry, University of Warwick, Coventry, UK, CV4 7AL.
[2] Warwick Medical School, University of Warwick, Coventry, UK, CV4 7AL.
[3] Jülich Centre for Neutron Science, Forschungszentrum Jülich GmbH, Lichtenbergstr. 1, Garching, 85747, Germany.
[4] Department of Materials Science & Metallurgy, University of Cambridge, Cambridge, UK, CB3 0FS.

Supporting Information Placeholder

ABSTRACT: Antifreeze glycoproteins from polar fish are the most potent ice recrystallization (growth) inhibitors known, and synthetic mimics are required for low temperature applications such as cell cryopreservation. Here we introduce facially amphipathic glycopolymers which mimic the 3-dimensional structure of AFGPs. Glycopolymers featuring segregated hydrophilic and hydrophobic faces were prepared by ring-opening metathesis polymerization and their rigid conformation was confirmed by small-angle neutron scattering. Ice recrystallization inhibition (IRI) activity was reduced when a hydrophilic oxo-ether was installed on the glycan-opposing face, but significant activity was restored by incorporating a hydrophobic dimethylfulvene residue. This biomimetic strategy demonstrates that segregated domains of distinct hydrophilicity/hydrophobicity are a crucial motif to introduce IRI activity, and increases our understanding of the complex ice crystal inhibition processes.

Antifreeze glycoproteins, AFGPs, are found in the tissues and blood serum of extremophile fish species, and act to modulate the growth of extracellular ice.[1] A key property of AFGPs is ice recrystallization inhibition, IRI, which slows ice crystal growth (distinct from nucleation[2]).[3] Ice recrystallization is a major cause of cell death during the freezing of cells and tissue for transfusion, fundamental biomedicine and cell biology. Hence, AFGPs (or their mimics) have many potential applications.[4] Cryopreservation with AFGPs (and non-glycosylated antifreeze proteins – AFPs)[5] is limited, however, by their secondary property of dynamic ice shaping, whereby the AFGPs shape the ice into needle-like (spicular) morphologies, which can pierce cell membranes.[3] AFGPs are also challenging to synthesize, by multistep procedures.[6,7] Gibson and coworkers have developed synthetic polymers[8,9] based upon poly(vinyl alcohol) and poly(ampholytes) which have been found to enhance the cryopreservation of blood,[10–12] and nucleated cells.[4,13]

In the case of AFPs, defined ice-binding faces have been identified using structural biology methods.[14] Conversely, there is no crystal structure available of AFGPs, and the exact structural motifs required for IRI are unknown, although the glycan unit is essential for ice shaping.[7] Solution NMR studies suggest that AFGPs form a polyproline II type helix, with the glycans on one face, and peptides on the opposite, forming a facially amphipathic structure.[15] It is emerging that this segregated display of hydrophobic/phillic groups, rather than a 'binding site' is the essential feature for IRI activity.[8,16,17] Molecular modelling recently revealed that the hydrophobic face, not the glycans, of AFGP interact with the ice, and that the spatial segregation along the polyproline II helix is essential.[18] Gibson and coworkers have shown that homo-polyproline has weak IRI,[4] and that self-assembled metallohelicies with 'patchy' amphipathy are potent IRIs,[19] which supports a hypothesis that well defined ice binding domains are not essential for IRI.[20] Amphipathy has also been seen to be important in ice nucleation.[21] This evidence suggests that IRI, but not ice shaping,[22] could be selectively introduced into new and emerging (bio)materials, if precise control over hydrophilic/phobic domains is possible. The design of polymers with solvent-exposed hydrophobic domains is, however, non-trivial. Block copolymeric amphiphiles spontaneously self-assemble into micelles/vesicles to reduce hydrophobic domain contact with water, and hence only 'water loving' surfaces are exposed.[23] Tew and coworkers have developed facially amphipathic cationic polymers, with opposing positive charges and lipophilic domains to mimic the function of antimicrobial peptides.[24,25] A crucial design step was the use of ring-opening metathesis polymerization, ROMP, which introduces rigid alkene backbones, whilst balancing the hydrophobicity/hydrophilicity to maintain both solubility and the

presentation of hydrophobic faces. These have shown particular potency as potential antimicrobials.[26]

Considering the above, we designed and synthesized locally-rigid, facially amphipathic glycopolymers. A combination of ice binding assays, modelling and small-angle neutron scattering (SANS) provides compelling evidence that local amphipathy is an essential motif for introducing IRI activity, providing design rules for new materials to mimic AFGP function.

Figure 1A shows the solution state structure of AFGP,[7] with the disaccharide units spatially segregated from the hydrophobic peptide backbone. Our approach was to use ROMP polymerization to introduce local rigidity,[27] compared to flexible backbones obtained from radical polymerization. Four monomers were synthesized to give a range of amphipathies: **M1** was prepared by acetylation of a commercial norbornene diol. **M2/3** were synthesized by Koenigs–Knorr coupling of acetobromo-α-D-galactose with *exo,exo*-[oxo/fulvene]norborneneimide. **M4** was synthesized by substitution of monomethoxyhexaethylene glycol monotosylate, Fig 1B. The hydrophilic galactose and hydrophobic fulvene motifs were selected in particular due to their intrinsic rigidities, giving monomers with structurally distinct domains of opposing polarity. These monomers were polymerized using Grubbs 3rd generation catalyst and acetate protecting groups removed by treatment with sodium methoxide followed by ion exchange, Fig 1C. The panel of amphipathic polymers were characterized by SEC (Đ < 1.4), NMR and IR (Supp. Info.), Table 1.

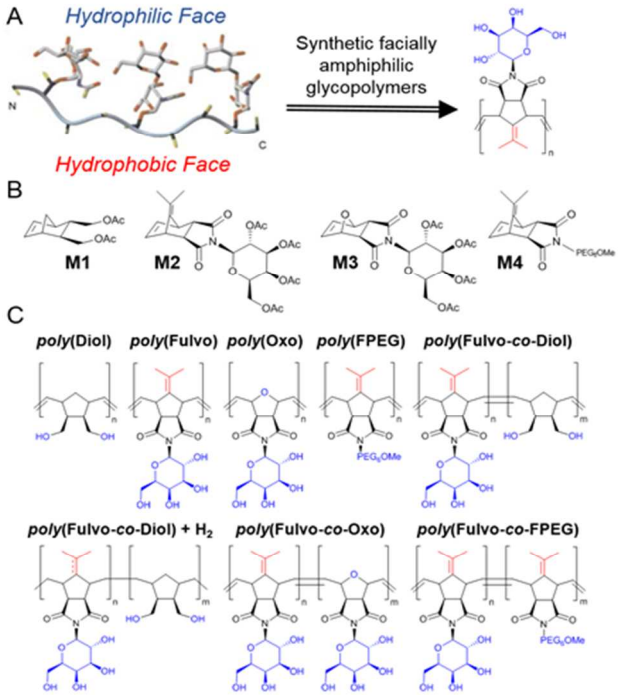

Fig 1 A) Concept of facially amphipathic ROMP polymers to mimic AFGP. Figure partially reproduced from Tachibana *et al.* (2004)[7] B/C) Monomers and polymers synthesized here; hydrophilic groups are indicated in blue, and hydrophobic in red.

The polymer library was assessed for IRI activity using a 'splat' assay: where ice crystals are nucleated and their growth after 30 minutes at –8 ºC is recorded. Activity is expressed as the mean grain area (MGA) relative to a PBS control, with smaller values representing more activity. Polymers derived from **M2** containing the 'fulvo' motif were significantly less soluble than those derived from **M3**, containing the 'oxo'-ether units. The solution concentrations of these were therefore determined by UV-Vis spectroscopy (Supp. Info for Beer-Lambert plots) at saturation. In the case of *poly*(Fulvo), 1% v/v DMSO was required and controls were adjusted to account for this.

Table 1 Polymer Characterization

	$M_{n(THEO)}$ (g.mol^{-1}) *[a]*	$M_{n\,(SEC)}$ (g.mol^{-1}) *[a]*	Đ (-) *[a]*	DP (-) *[a]*	Conv % *[b]*
		2200	1.01	14	
***poly*(Diol)** *[c]*	10,000	5300	1.01	34	100
		8,400	1.02	54	
***poly*(Fulvo)**	25,000	10,300	1.21	28	100
***poly*(Oxo)**	10,000	7,300	1.18	22	100
***poly*(FPEG)**	10,000	35,900	1.38	133	100
***poly*(Fulvo-*co*-Diol)-11**	5,000	10,700	1.12	14,35	94/97
***poly*(Fulvo-*co*-Diol)-17**	10,000	16,800	1.10	22,54	100
***poly*(Fulvo-*co*-Diol)-35**	25,000	34,600	1.26	47,112	100
***poly*(Fulvo-*co*-Oxo)**	10,000	7,700	1.35	11,11	100/96
***poly*(Fulvo-*co*-FPEG)**	10,000	55,600	1.47	76,58	71

[a] Determined by SEC. *[b]* Determined by ^{1}H NMR. *[c]* Single species.

Poly(Oxo) was found to inhibit ice crystal growth by approximately 50% MGA at concentrations above 5 mg.mL^{-1}, Fig 2A, which is more active than many previously reported IRI active polymers.[28,29] The *poly*(Fulvo) derivative featuring the hydrophobic face, however, was considerably more activity, inhibiting by ~ 50% MGA at just 0.5 mg.mL^{-1} (solubility limit), supporting the facially amphipathic hypothesis for IRI. Molecular models corroborate this (Fig 2B), and illustrate the relative increase in hydrophobicity across the *poly*(Oxo) and *poly*(Fulvo) homopolymers. To improve the solubility, a 1:1 statistical copolymer of **M2**/**M3**, *poly*(Fulvo-*co*-Oxo), was prepared. This co-polymer had significantly improved solubility and comparable overall IRI activity to *poly*(Fulvo) showing that some co-monomer incorporation is tolerated, unlike PVA,[30] and example ice wafers are shown in Fig 2C. However the non-ideal copolymerization kinetics of the oxo (**M2**) and fulvo (**M3**) co-monomers will have led to a blocky, rather than statistical copolymerization.[31,32] Infrared analysis confirmed incomplete acetate removal (in contrast to the homo polymers), suggesting an internalized domain structure and/or aggregation, with some (hydrophobic) surfaces being solvent inaccessible and hence limiting the total activity *poly*(Fulvo-*co*-Oxo). The monomers alone also had no activity (Supp. Info), confirming that a macromolecular architecture is essential.

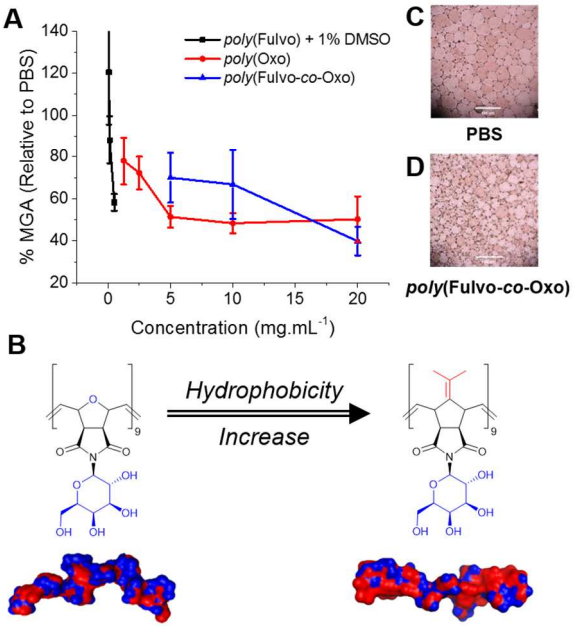

Fig 2 A) IRI activities of the *poly*(Fulvo), (Oxo), and copolymer series. B) Hydrophobic surface map of *poly*(Fulvo) and (Oxo) C/D) Ice crystal wafer of PBS and *poly*(Fulvo-*co*-Oxo).

To improve solubility, a norbornene diol monomer, **M1**, with a non-hydrophilic bridgehead was investigated. Deacetylated homopolymers of **M1**, *poly*(Diol), were found to have surprisingly low solubility and no activity at their solubility limit of 0.5 mg.mL^{-1}. However, when **M1** was incorporated as a co-monomer with the (IRI active) 'fulvo' monomer **M2** to give *poly*(Fulvo-*co*-Diol), an overall increase in solubility was achieved. *Poly*(Fulvo-*co*-Diol)-17 had remarkable IRI activity; 40% MGA at just 1.3 mg.mL^{-1}, Fig 3. This polymer showed some molecular weight dependence on activity, with 17 kDa having more activity than 11 kDa (and far more than the monomer, indicating the need for a macromolecular architecture). Increasing the molecular weight further to 35 kDa lowered the solubility of the copolymer, and hence activity, highlighting a 'sweet spot'. Work undertaken by Inada *et. al.* described the molecular weight dependence on IRI of PVA. [33] Similarly, a previous study by Deswal *et. al* reported on the IRI activity of proteins extracted from the leaves of the freeze tolerant plant Seabuckthorn, of which superior antifreeze activity was observed only for polypeptides of elevated molecular weights.[34] Replacing the glycan with a short oligo(ethylene glycol), PEG, chain to give both *poly*(Fulvo-*co*-FPEG) and *poly*(FPEG), decreased activity as the (flexible) PEG can access numerous conformations, reducing the overall amphipathy. See ESI. Hydrogenation of the alkene backbone to increase flexibility resulted in a wholly insoluble polymer. See ESI. These observations demonstrate that precise macromolecular engineering is essential to achieve a potent IRI mimetic.

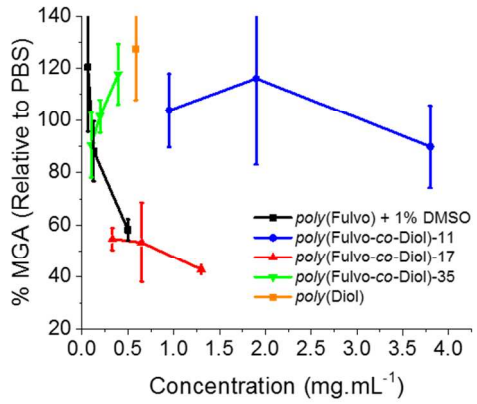

Fig 3 IRI activities of the *poly*(Fulvo-*co*-Diol) molecular weight series

AF(G)Ps bind to specific ice crystal faces,[35,36] leading to dynamic ice shaping (unwanted in cryopreservation[3]). Control ice crystals (Fig 4A) showed no dynamic ice shaping, but addition of AFGPs (Fig 4B) produced distinctive spicular (needle-like) crystals. *Poly*(Fulvo-*co*-Diol) (Fig 4C) did not lead to ice shaping, ruling out strong and specific ice face recognition and showing that these effects can be separated by macromolecular design.

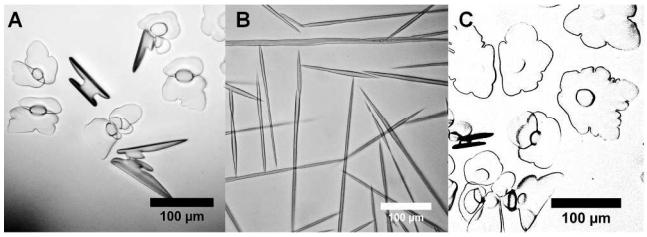

Fig 4 Ice morphology analysis. A) Water (-6 °C); B) AFGP-8 (-5 °C); C) *poly*(Fulvo-*co*-Diol)-17 [0.72 mg.mL^{-1}] (-8 °C).

SANS was employed to evaluate the solution conformation and rigidity of the *poly*(Fulvo-*co*-Diol) series, Fig 5 (and Supp. Info). The persistence lengths, b_t, were estimated from the position of the characteristic crossover between the scattering profile typical for fractal aggregates ($q^{-3.5}$) to that of rigid rods (q^{-1}) (see the ESI). [37,38] The estimated b_t values for *poly*(Fulvo-*co*-Diol)-11 and *poly*(Fulvo-*co*-Diol)-17 are 38.9 and 44.4 Å, respectively. It should be noted that the overlap may actually occur at a lower *q* region, but is masked by aggregate scattering. Thus, these values should be taken as the minimum persistence lengths for each polymer. Nevertheless, each b_t is much larger than the monomer length (~10 Å) which suggests that the chain backbones are locally stiff.[38] Furthermore, given the approximate contour length, *L*, of both polymer chains (490 Å and 760 Å for *poly*(Fulvo-*co*-Diol)-11 and *poly*(Fulvo-*co*-Diol)-17, respectively), the large b_t suggests rigid rather than highly flexible aggregates, of potentially rod-like structures. This rigidity coupled with the intrinsic amphipathy of the polymers is aligned with the hypothe-

sized semi-rigid (and generally amphipathic) ice binding faces of AFPs,[14,39] and the flexible hydrophilic 'glycan face' of AFGPs, providing evidence that facial amphipathy is a key motif for introducing IRI activity into a diverse range of polymers.

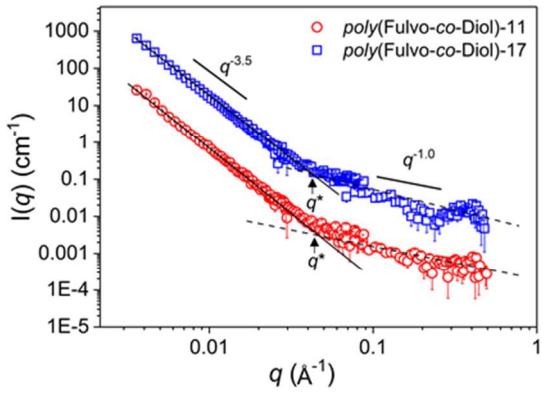

Fig 5 SANS data for *poly*(Fulvo-*co*-Diol)-11 (100%, red) and *poly*(Fulvo-*co*-Diol)-17 (100%, blue) in D_2O at 25 °C. Straight lines show -3.5 and -1 decays for comparison.

To conclude, we have designed and synthesized facially amphipathic glycopolymers to mimic the solution confirmation and selective functions of antifreeze glycoproteins. It was found that the addition of hydrophobic faces, opposing the glycan units, introduced potent IRI activity, but that substitution with a more hydrophilic ether unit removed activity. These results support a mechanism for IRI activity which is dependent upon local water ordering rather than an essential ice binding unit, and there was no evidence of dynamic ice shaping; with small angle neutron scattering supporting a locally rigid confirmation, as seen for AF(G)Ps, supporting the hypothesis of amphipathy as the driver for activity.

ASSOCIATED CONTENT

Supporting Information.

Full experimental details, including synthesis/characterization, additional IRI data and SANS analysis is in the Supporting Information. This material is available free of charge via the Internet at http://pubs.acs.org.

AUTHOR INFORMATION

Corresponding Author

Prof. Matthew I. Gibson, m.i.gibson@warwick.ac.uk.

Notes

No competing financial interests have been declared.

ACKNOWLEDGMENT

MIG holds an ERC Starter Grant (CRYOMAT 638661). Thanks to A. L. DeVries for supplying the antifreeze glycoprotein AFGP-8. The SANS portion of this work is based upon experiments performed at the KWS-2 instrument operated at the Heinz Maier-Leibnitz (MLZ), Garching, Germany.

REFERENCES

(1) Harding, M. M.; Anderberg, P. I.; Haymet, A. D. J. *Eur. J. Biochem.* **2003**, *270* (7), 1381.
(2) Congdon, T.; Dean, B. T.; Kasperczak-Wright, J.; Biggs, C. I.; Notman, R.; Gibson, M. I. *Biomacromolecules* **2015**, *16* (9), 2820.
(3) Chao, H.; Davies, P. L.; Carpenter, J. F. *J. Exp. Biol.* **1996**, *199* (Pt 9), 2071.
(4) Graham, B.; Bailey, T. L.; Healey, J. R. J.; Marcellini, M.; Deville, S.; Gibson, M. I. *Angew. Chem. Int. Ed.* **2017**, *56*, 15941.
(5) Davies, P. L. *Trends in Biochemical Sciences*. Elsevier November 2014, pp 548–555.
(6) Wilkinson, B. L.; Stone, R. S.; Capicciotti, C. J.; Thaysen-Andersen, M.; Matthews, J. M.; Packer, N. H.; Ben, R. N.; Payne, R. J. *Angew. Chem. Int. Ed.* **2012**, *51* (15), 3606.
(7) Tachibana, Y.; Fletcher, G. L.; Fujitani, N.; Tsuda, S.; Monde, K.; Nishimura, S. I. *Angew. Chemie - Int. Ed.* **2004**, *43* (7), 856.
(8) Biggs, C. I.; Bailey, T. L.; Ben Graham; Stubbs, C.; Fayter, A.; Gibson, M. I. *Nat. Commun.* **2017**, *8* (1), 1546.
(9) Gibson, M. I. *Polym. Chem.* **2010**, *1* (8), 1141.
(10) Deller, R. C.; Vatish, M.; Mitchell, D. A.; Gibson, M. I. *Nat. Commun.* **2014**, *5*, 3244.
(11) Mitchell, D. E.; Cameron, N. R.; Gibson, M. I. *Chem. Commun.* **2015**, *51* (65), 12977.
(12) Mitchell, D. E.; Lovett, J. R.; Armes, S. P.; Gibson, M. I. *Angew. Chemie - Int. Ed.* **2016**, *55* (8), 2801.
(13) Deller, R. C.; Pessin, J. E.; Vatish, M.; Mitchell, D. A.; Gibson, M. I. *Biomater. Sci.* **2016**, *47*, 935.
(14) Strom, C. S.; Liu, X. Y.; Jia, Z. *J. Biol. Chem.* **2004**, *279* (31), 32407.
(15) Nguyen, D. H.; Colvin, M. E.; Yeh, Y.; Feeney, R. E.; Fink, W. H. *Biophys. J.* **2002**, *82* (6), 2892.
(16) Capicciotti, C. J.; Leclere, M.; Perras, F. A.; Bryce, D. L.; Paulin, H.; Harden, J.; Liu, Y.; Ben, R. N. *Chem. Sci.* **2012**, *3* (5), 1408.
(17) Capicciotti, C. J.; Kurach, J. D. R.; Turner, T. R.; Mancini, R. S.; Acker, J. P.; Ben, R. N. *Sci. Rep.* **2015**, *5*, 9692.
(18) Mochizuki, K.; Molinero, V. *J. Am. Chem. Soc.* **2018**, 10.1021/jacs.7b13630.
(19) Mitchell, D. E.; Clarkson, G.; Fox, D. J.; Vipond, R. A.; Scott, P.; Gibson, M. I. *J. Am. Chem. Soc.* **2017**, *139* (29), 9835.
(20) Geng, H.; Liu, X.; Shi, G.; Bai, G.; Ma, J.; Chen, J.; Wu, Z.; Song, Y.; Fang, H.; Wang, J. *Angew. Chem. Int. Ed.* **2017**, *56* (4), 997.
(21) Liu, K.; Wang, C.; Ma, J.; Shi, G.; Yao, X.; Fang, H.; Song, Y.; Wang, J. *Proc. Natl. Acad. Sci.* **2016**, *113* (51), 14739.
(22) Leclère, M.; Kwok, B. K.; Wu, L. K.; Allan, D. S.; Ben, R. N. *Bioconjug. Chem.* **2011**, *22* (9), 1804.
(23) Mai, Y.; Eisenberg, A. *Chem. Soc. Rev.* **2012**, *41* (18), 5969.

(24) Ilker, M. F.; Nüsslein, K.; Tew, G. N.; Coughlin, E. B. *J. Am. Chem. Soc.* **2004**, *126* (48), 15870.
(25) Arnt, L.; Tew, G. N. *J. Am. Chem. Soc.* **2002**, *124* (26), 7664.
(26) Lienkamp, K.; Madkour, A. E.; Musante, A.; Nelson, C. F.; Nüsslein, K.; Tew, G. N. *J. Am. Chem. Soc.* **2008**, *130* (30), 9836.
(27) Colak, S.; Nelson, C. F.; Nusslein, K.; Tew, G. N. *Biomacromolecules* **2009**, *10* (2), 353.
(28) Stubbs, C.; Lipecki, J.; Gibson, M. I. *Biomacromolecules* **2017**, *18* (1), 295.
(29) Capicciotti, C. J.; Trant, J. F.; Leclère, M.; Ben, R. N. *Bioconjug. Chem.* **2011**, *22* (4), 605.
(30) Congdon, T.; Notman, R.; Gibson, M. I. *Biomacromolecules* **2013**, *14* (5), 1578.
(31) Kiessling, L. L.; Strong, L. E. In *Alkene Metathesis in Organic Synthesis*; Fuerstner, A., Ed.; Springer-Verlag: Berlin Heidelberg, 2013; pp 219–220.
(32) Tallon, M. A. In *Handbook of Maleic Anhydride Based Materials*; Musa, O. M., Ed.; Springer International Publishing: Switzerland, 2016; pp 387–388.
(33) Inada, T.; Lu, S. S. *Cryst. Growth Des.* **2003**, *3* (5), 747.
(34) Deswal, R.; Gupta, R.; Sharma, B. *J. Proteins Proteomics* **2016**, *7* (3), 199.
(35) Raymond, J. A.; Wilson, P.; DeVries, A. L. *Proc. Natl. Acad. Sci. U. S. A.* **1989**, *86* (3), 881.
(36) Knight, C. A.; Driggers, E.; DeVries, A. L. *Biophys. J.* **1993**, *64* (1), 252.
(37) Schmidt, M.; Paradossi, G.; Burchard, W. *Makromol. Chem. Rapid Commun.* **1985**, *6* (11), 767.
(38) Buhler, E.; Boué, F. *Macromolecules* **2004**, *37* (4), 1600.
(39) Howard, E. I.; Blakeley, M. P.; Haertlein, M.; Haertlein, I. P.; Mitschler, A.; Fisher, S. J.; Siah, A. C.; Salvay, A. G.; Popov, A.; Dieckmann, C. M.; Petrova, T.; Podjarny, A. *J. Mol. Recognit.* **2011**, *24* (4), 724.

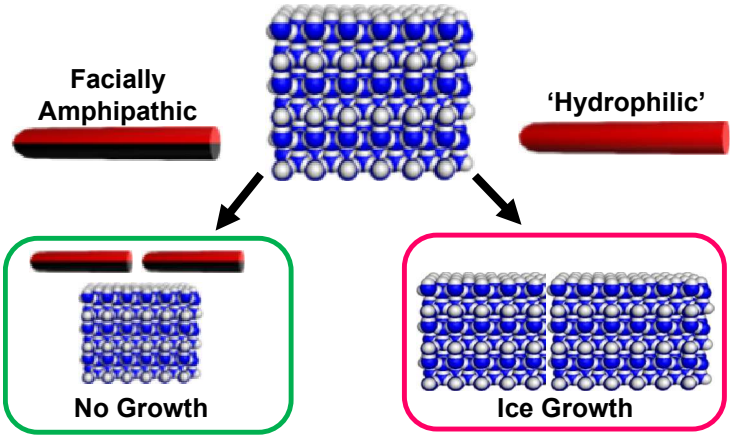
Facially
Amphipathic
'Hydrophilic'
No Growth
Ice Growth

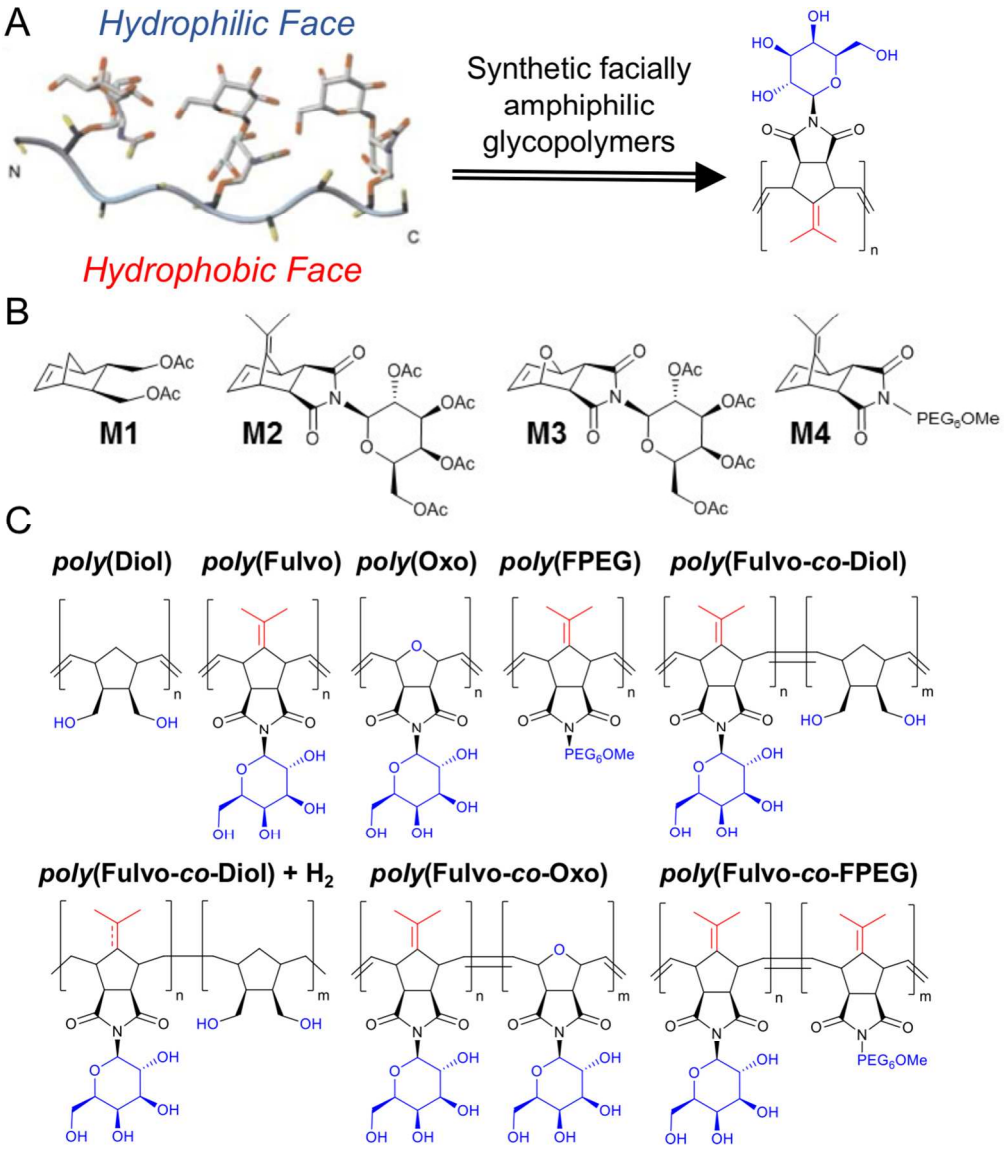

Figure 1

163x185mm (225 x 225 DPI)

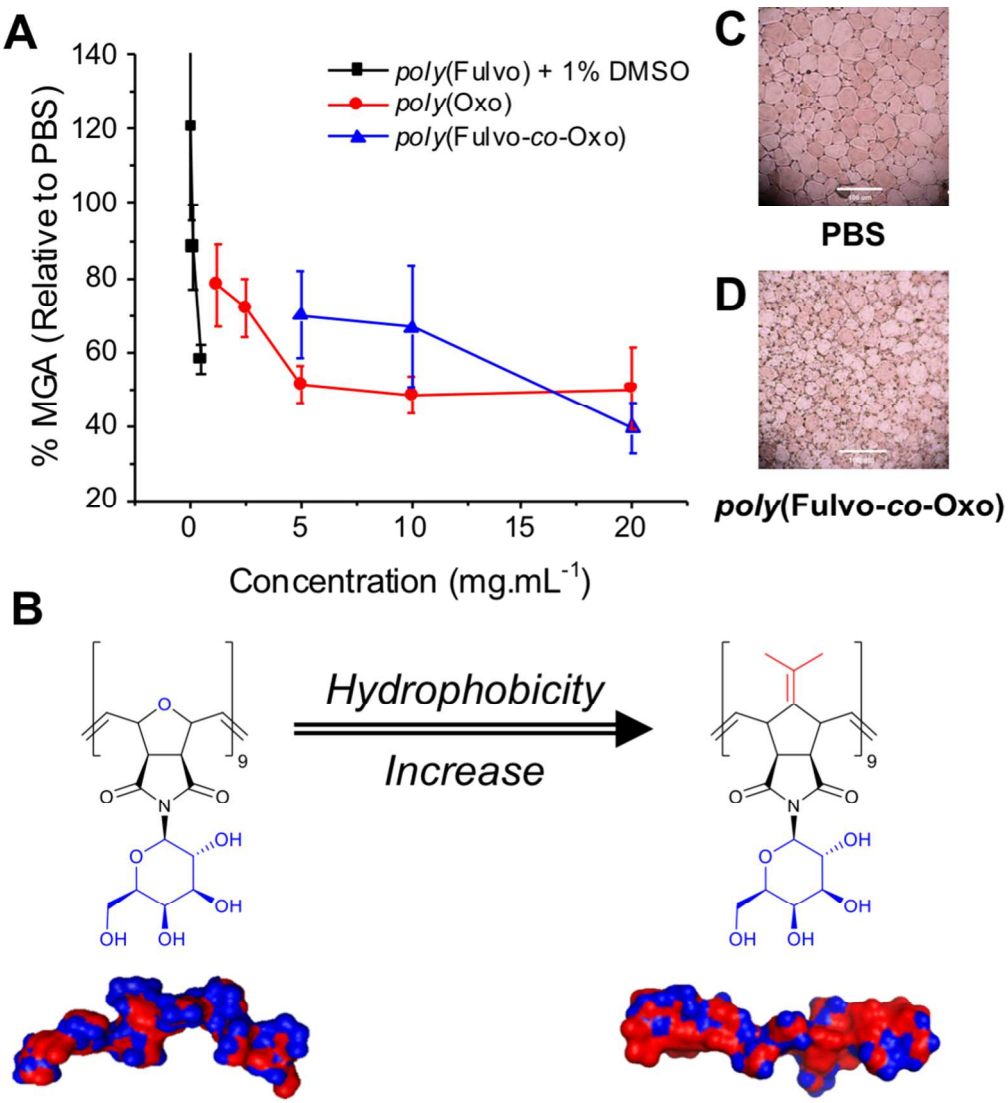

Figure 2

133x146mm (225 x 225 DPI)

Figure 3.

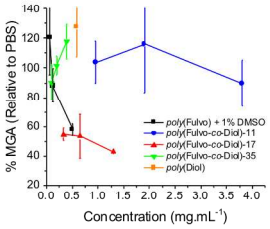

Figure 3

338x190mm (225 x 225 DPI)

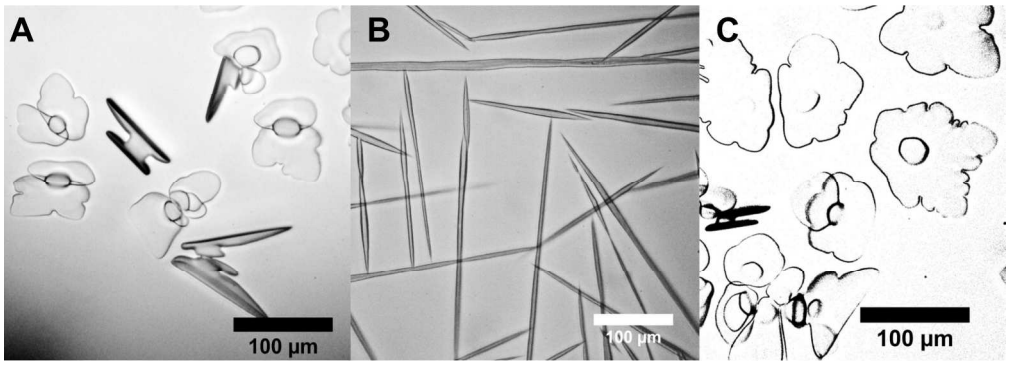

Figure 4

334x118mm (225 x 225 DPI)

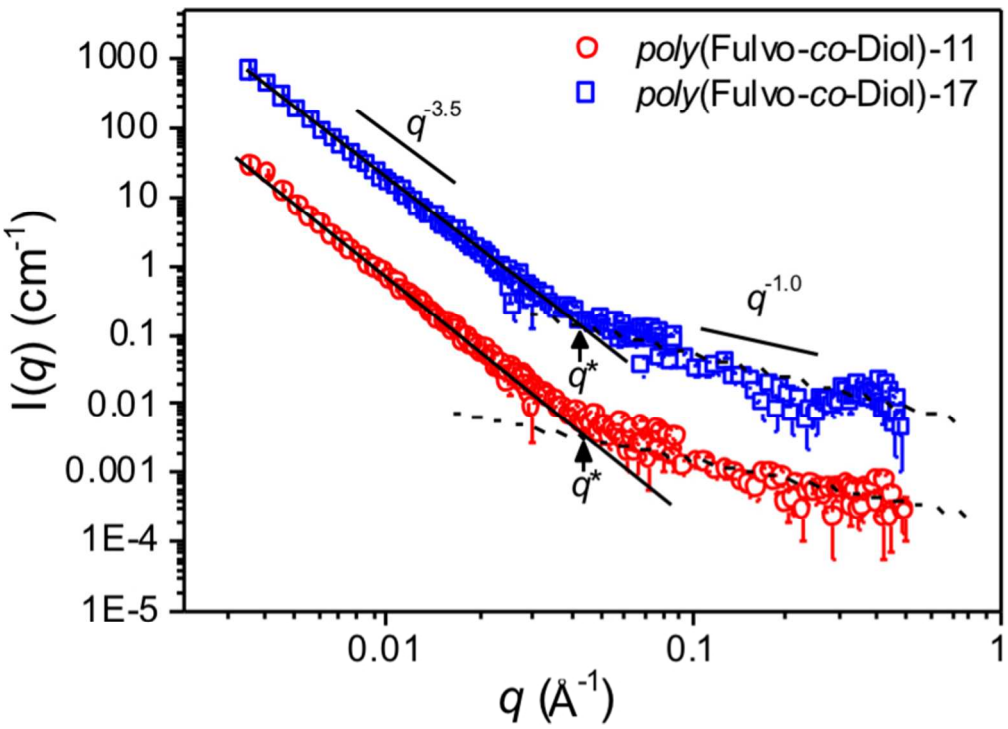

Figure 5

96x69mm (225 x 225 DPI)

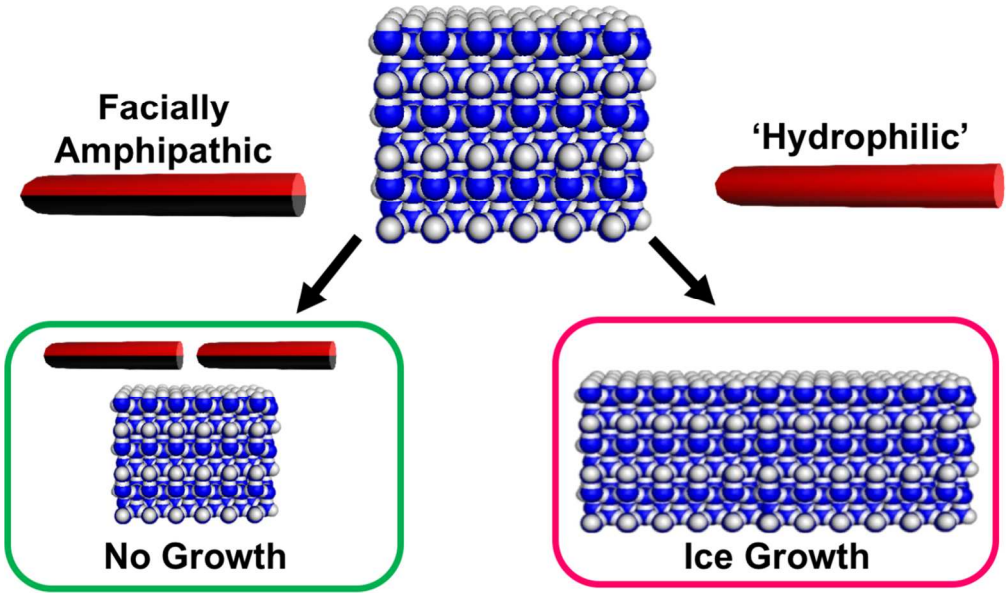

Table of Contents Image

156x92mm (225 x 225 DPI)